Freezing-thawing processes in glass fiber board
Hokoi, S.; Hatano, M.; Matsumoto, M.; Kumaran, M. K.

National Research Council Canada   Conseil national de recherches Canada

Canada

Freezing-thawing processes in glass fiber board

NRCC-44289

Hokoi, S.; Hatano, M.; Matsumoto, M.; Kumaran, M.K.

July 2000

National Research Council Canada   Conseil national de recherches Canada

Freezing-Thawing Processes in Glass Fiber Board

S. HOKOI[1]

Department of Architecture and Environmental Design
Graduate School of Engineering
Kyoto University
Yoshida-Honmachi, Sakyo-ku
Kyoto 606-8501, Japan

M. HATANO

Government of Housing Loan Corporation
2-10-8 Bancho
Takamatsu 761-8076, Japan

M. MATSUMOTO

School of Engineering
Osaka-Sangyo University
3-1-1 Nakagaito, Daito
Osaka 574-0013, Japan

M. K. KUMARAN

Building Envelope and Structure
Institute for Research in Construction
National Research Council of Canada
1500 Montreal Road
Ottawa, Ontario, K1A 0R6, Canada

ABSTRACT: For the prevention of vapor condensation and accompanying damage in cold regions, the behavior of water and ice in porous materials should be understood. In this study, experiments on the freezing-thawing processes in a glass fiber board, which is a typical insulation, were conducted. The freezing-thawing processes were analyzed with the use of simultaneous heat and moisture transfer equations that accounted for the existence of ice.

[1]Author to whom correspondence should be addressed. E-mail: hokoi@archi.kyoto-u.ac.jp

The result of the analysis agrees well with that of the experiment. In materials with large pores such as glass fiber board, the moisture transfers mainly in the gaseous phase. As a result, the maximum ice content is found at the colder boundary of the wall, which differs from the result in our previous investigation [1] for Leda Clay with pores that are much smaller.

KEY WORDS: vapor condensation, heat and moisture transfer, freezing-thawing, transport properties, glass fiberboard.

INTRODUCTION

WHILE VAPOR CONDENSATION on inner wall surfaces has been decreasing due to appropriate thermal insulation and designs aimed at preventing condensation damage, the possibility of condensation within the walls at other locations may be increasing. Especially in cold regions, liquid water may freeze in porous building materials and cause serious damage. In order to avoid condensation damage, the transient effects of the condensation-evaporation and freeze-thaw in materials should be predicted. From such a point of view, a basic theory on freezing-thawing processes has been proposed, and analytical examples with respect to soil and snow have been shown [2,3]. A numerical model, employing a local-averaging formulation, was developed for heat transfer and water vapor deposition within fiberglass insulation under exfiltration and frosting conditions [4]. Frost growth on the surface was modeled using special frost boundary conditions. Non-isotropic permeability effects that occur in fiberglass boards were included in the model for porous flow.

In our previous paper [1], the freezing-thawing processes in a wall made of Leda Clay were analyzed. Under a constant external temperature, an ice accumulation occurs at a region where the temperature is around 0°C. To the contrary, the ice content becomes quite high at the outer region with the temperature much lower than 0°C when the external temperature changes cyclically. The present paper reports the experimental results on freezing-thawing processes in glass fiberboard, a typical insulation material. The results are analyzed by making use of simultaneous heat and moisture transfer equations that take into account the existence of ice. Karagiozis et al. [5] made a similar analysis based on the present experiments and showed the importance of two- and three-dimensional analysis.

Because glass fiberboard has large pores, and thus moisture moves mainly in gaseous form up until high moisture content, it is expected to show different thermal and hygric behaviors from the wall made of soil. Furthermore, the influence of material properties, such as vapour permeability and moisture diffusivity, on the freezing process is examined. The present results could be used effectively for understanding and improving the existing test methods such as ASTM C666 [6] for durability of building materials.
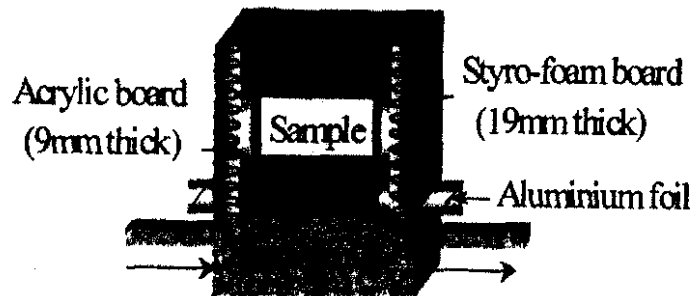
Figure 1. *Schematic of experimental setup.*

FREEZING-THAWING EXPERIMENT ON GLASS FIBERBOARD

Freezing Process

The test specimen was a 10 cm × 10 cm × 10 cm glass fiberboard with the density of 48 kg/m^3. The four sides of the sample were made vapor-tight by acrylic plates and the bottom by an aluminum plate as shown in Figure 1. Nineteen mm thick extruded polystyrene plates also insulated the sides of the sample. The top surface was exposed to the ambient air of 20°C and 60% RH.

From time zero, cold refrigerant with a constant temperature of −10°C was flowed through the water bath under the aluminum plate. Water vapor flowed into the sample from the ambient air through the upper surface and condensed near the bottom, and a part of it also froze there. The moisture content distribution within

Figure 2. *Measured total moisture (liquid water + ice) content distribution during freezing process.*
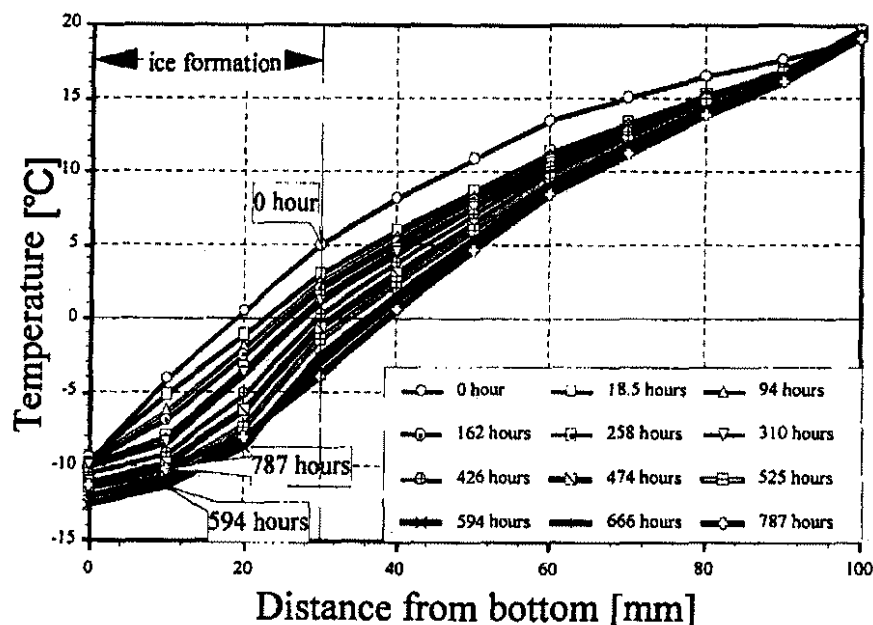
Figure 3. *Measured temperature distribution during freezing process.*

the test specimen was measured using a gamma-ray spectrometer at an interval of 2 mm [7].

Figure 2 shows the measured total moisture content distribution in the glass fiberboard. The moisture content increases from the bottom side with time. After 500 hours, a detectable "kink" appeared in the moisture content profile at 9 mm to 15 mm from the bottom.

The measured temperature distribution that corresponded to the moisture distributions is shown in Figure 3. As the freezing proceeded, the temperature decreased until the 594th hour. The profile is convex upward as a whole. The temperature gradient near the bottom is gradual compared with those in other regions and the temperature increases after 594 hours (about 25 days). This is probably due to the decrease in thermal resistance in the bottom region with the freezing process.

Thawing Process

The thawing experiment was started after the freezing experiment by heating the refrigerant up to 32°C. Figure 4 shows the measured distribution of the moisture content during the thawing process. As the ice melts and evaporates, the total amount of moisture contained in the sample decreases.

The corresponding measured temperature distribution is shown in Figure 5. In a region of 10 to 20 mm from the bottom, the temperature lower than 0°C is kept for a fairly long time. This seems to indicate that the ice remained there longer
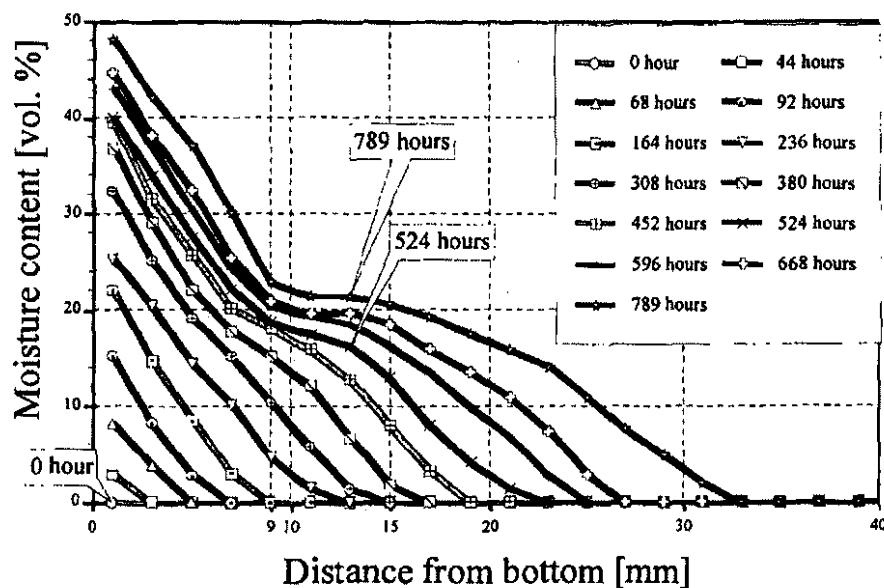
Figure 4. *Measured total moisture (liquid water + ice) content distribution during thawing process.*

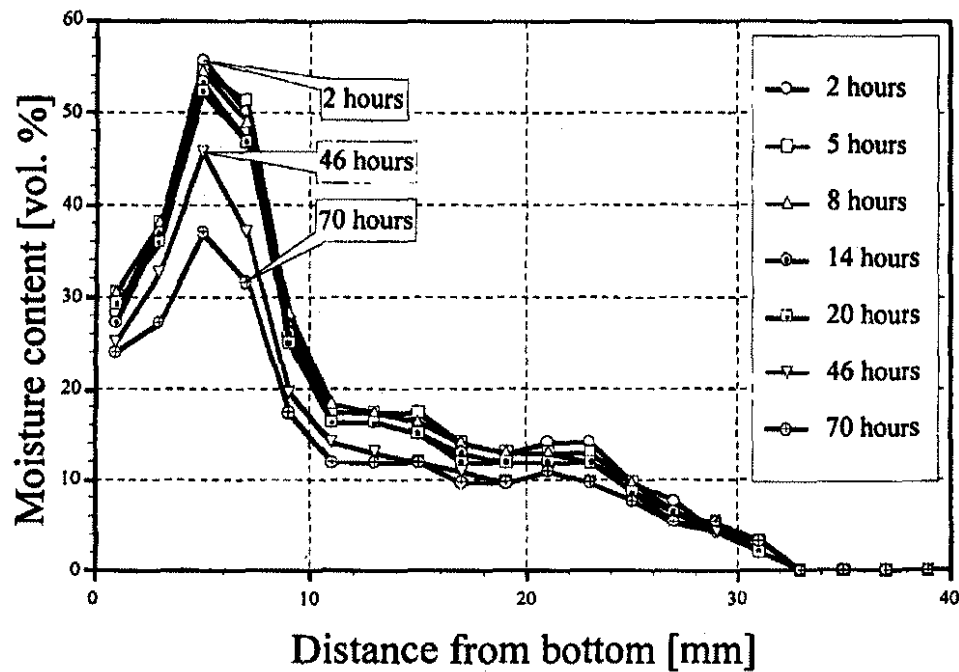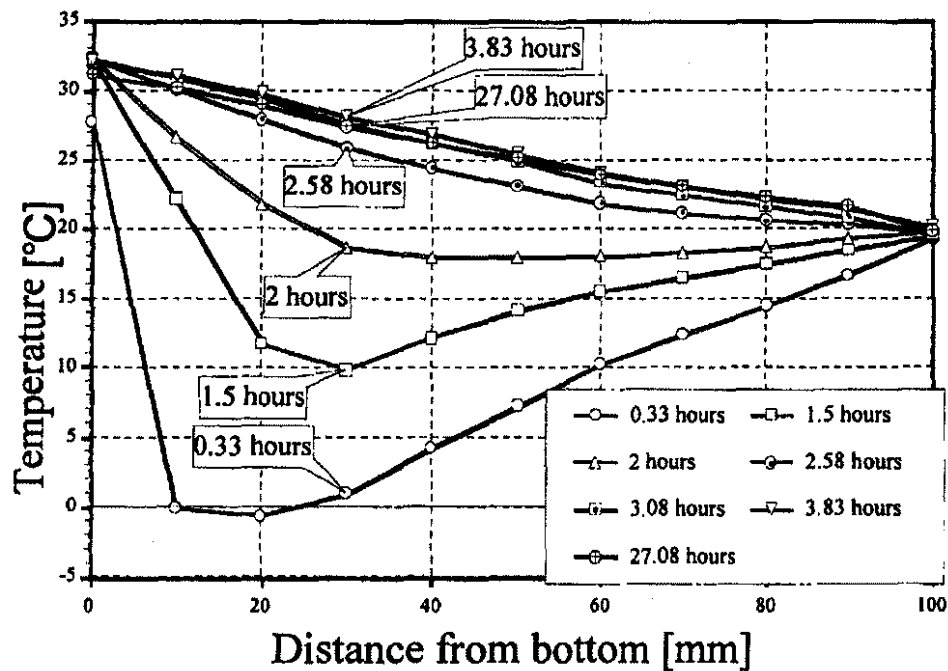**Figure 5.** *Measured temperature distribution during thawing process.*

than at any other region. After one and a half hours, the temperature became higher than 0°C everywhere else. The thawing rate is high compared with that of the freezing.

ANALYSIS OF FREEZING-THAWING PROCESSES

The experiment was analyzed by making use of the governing equations used in the previous paper [1].

Fundamental Equations [2,8]

Freezing-thawing processes are dealt with as a three-phase system including gaseous, liquid and solid phases. Under the following assumptions:

1. Each coexisting phase of moisture in the porous media is in local equilibrium; i.e., $\mu = \mu_g = \mu_l = \mu_i$.
2. The deformation of the microporous structure caused by the ice content change can be neglected during the freezing and thawing processes.
3. All variables are single valued; i.e., hysteresis and over-cooling are not present, the governing equations are derived.

Moisture balance:

$$\frac{\partial \rho_w \psi_w}{\partial t} = \nabla \cdot (\lambda'_{Tg} \nabla T) + \nabla \cdot \{(\lambda'_{\mu g} + \lambda'_{\mu l}) \nabla \mu\} \tag{1}$$

Energy balance:

$$c\rho\psi \frac{\partial T}{\partial t} = \nabla \cdot (\lambda \nabla T) + H_{gl}\{\nabla \cdot (\lambda'_{Tg} \nabla T) + \nabla \cdot (\lambda'_{\mu g} \nabla \mu)\} + H_{li} \frac{\partial \rho_i \psi_i}{\partial t} \tag{2}$$

where

$$\psi_s + \psi_g + \psi_l + \psi_i = 1 \tag{3}$$

$$\rho_w \psi_w = \rho_g \psi_g + \rho_l \psi_l + \rho_i \psi_i \tag{4}$$

$$c\rho\psi = c_s \rho_s \psi_s + c_g \rho_g \psi_g + c_l \rho_l \psi_l + c_i \rho_i \psi_i \tag{5}$$

and

ρ = density [kg/m^3]
ψ = volume fraction [m^3/m^3]
t = time [s]

T = absolute temperature [K]

μ = chemical potential of pore water relative to water as a one-com-
ponent system [J/kg]

c = specific heat [J/kgK]

$\lambda'_{\mu g}, \lambda'_{\mu l}, \lambda'_{\mu}$ = moisture conductivities in gaseous, liquid and total phase related
to water chemical potential gradient [kg/ms(J/kg)]

$\lambda'_{Tg}, \lambda'_{Tl}, \lambda'_{T}$ = moisture conductivities in gaseous, liquid and total phase related
to temperature gradient [kg/msK]

λ = thermal conductivity [W/mK]

H = heat of phase change, vapour-liquid or solid-liquid [J/kg]

∇ = divergent

Suffix w = water, g = gas, l = liquid, i = ice, s = solid matrix of the glass fibre
board.

Freezing Point Depression and Equilibrium Liquid Moisture Content [2,8]

Under a local equilibrium state of moisture in a three-phase system, the follow-
ing equation in terms of chemical potential relative to free water can be derived
from the Gibbs-Duhem relation with a few assumptions.

$$\mu = H_{li} \log_e \left(\frac{T}{T_o} \right) \tag{6}$$

where T_o is freezing temperature of free water at 273.16 K.

By taking the freezing process as an example (Figure 6), Equation (6) is ex-
plained. Equation (6) can be used to judge whether a material with a potential μ_a
under a non-freezing condition will freeze when it is brought into a colder environ-
ment below 0°C with temperature T_a.

If

$$\mu_a < H_{li} \log_e \left(\frac{T_a}{T_o} \right)$$

freezing does not occur even if T_a is below 0°C. Freezing begins when T_a decreases
to a temperature T calculated using Equation (6) with $\mu = \mu_a$. When the tempera-
ture is further decreased to T_b, then the liquid moisture content becomes ψ_b and the
difference ($\psi_a - \psi_b$) freezes.

Equation (6) shows that water chemical potential in a porous medium is a func-
tion of only the temperature in the freezing regime. When the moisture content of
the liquid phase (unfrozen liquid water content) is a single-valued function of the
water chemical potential, the governing equations (1) and (2) can be solved with
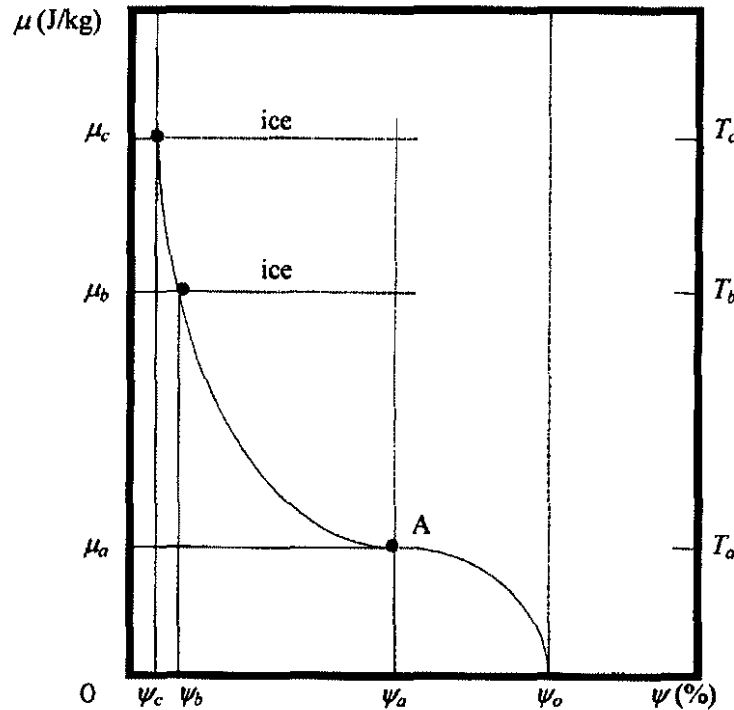
Figure 6. Equilibrium relationship among liquid moisture content, chemical potential and temperature.

respect to the unknown dependent variables T and μ_j. In the following analysis, it is assumed that an equilibrium relationship between the unfrozen liquid moisture content and potential below 0°C is the same as the relation above 0°C [8].

System Analyzed and Method of Analysis

A sample of 10 cm × 10 cm glass fiber is analyzed. Heat and moisture flow through the sample is regarded as one-dimensional in an initial set of simulations and as two-dimensional in the rest. In the two-dimensional analysis, the heat and moisture transfer in the vertical and horizontal directions. Whereas the heat flux through the side surfaces of the sample is taken into account, no moisture flow is assumed through the bottom and the side surfaces. The third kind of boundary condition is used on the upper surface with prescribed heat and mass transfer coefficients.

The governing equations are solved by an explicit finite difference method. The sample is divided into 25 slices with thickness of 4 mm in the vertical direction, while divided into 5 slices (× 2) of 10 mm thickness horizontally by taking into account the symmetry in the two-dimensional calculation.

The physical properties of the glass fiberboard in References [9,10] are used.

<div align="center">

ONE-DIMENSIONAL ANALYSIS OF
FREEZING-THAWING PROCESSES

</div>

In this section, a one-dimensional analysis is used for understanding the general nature of the physical processes. In order to have better agreement with the experimental results, a two-dimensional calculation is carried out in the next section.

Analysis of Freezing Process

COMPUTATIONAL CONDITIONS

As the boundary condition at the bottom, the measured refrigerant temperature is used which falls from 5°C to about −10°C in 60 minutes, while the temperature and chemical potential of the ambient air are kept constant. The relative humidity of the air is 60%. As initial conditions, temperatures at the upper and bottom surfaces are set at 20°C and 0°C, respectively. A linear temperature profile is assumed between the two surfaces. The heat transfer coefficient at the bottom surface is set at 23.3 [W/m²K] to accommodate the high thermal conductivity of the aluminum sheet.

RESULTS AND DISCUSSIONS

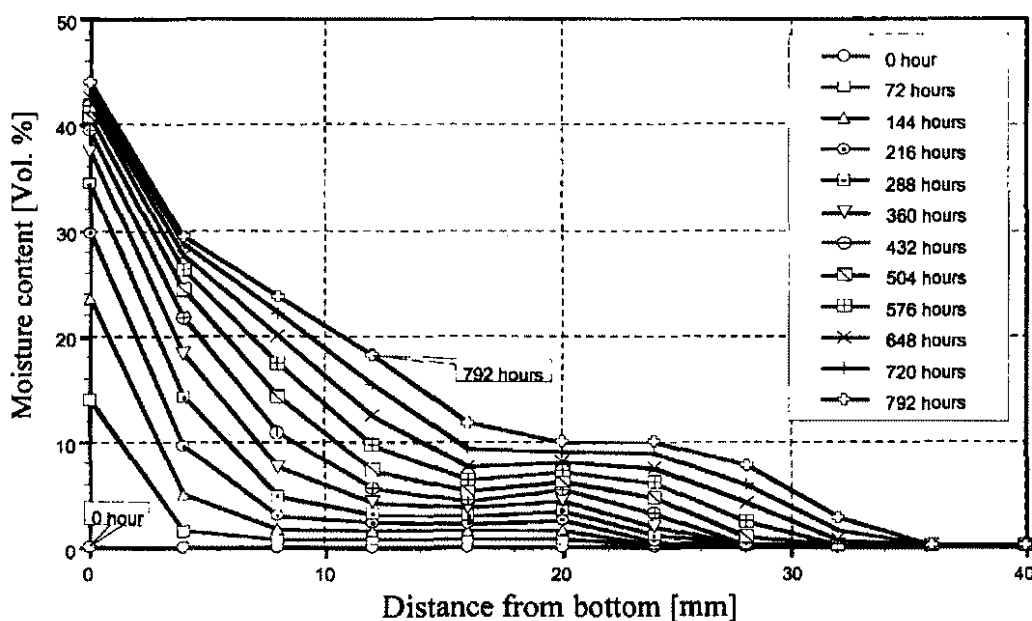Figure 7 shows the time history of the total moisture content. It predicts fairly

Figure 7. *Calculated total moisture (liquid water + ice) content distribution during freezing process.*
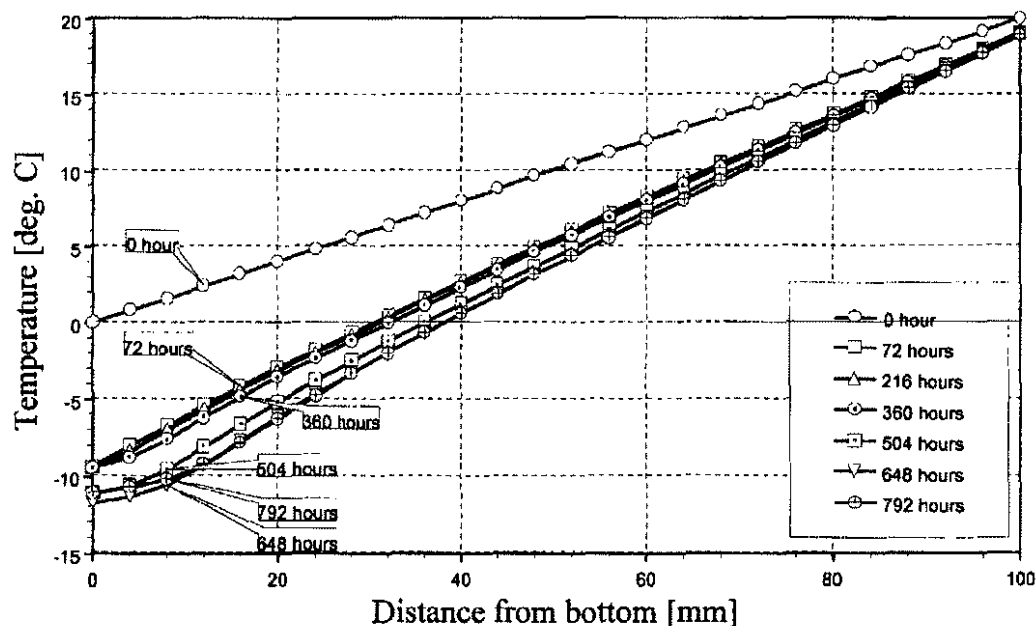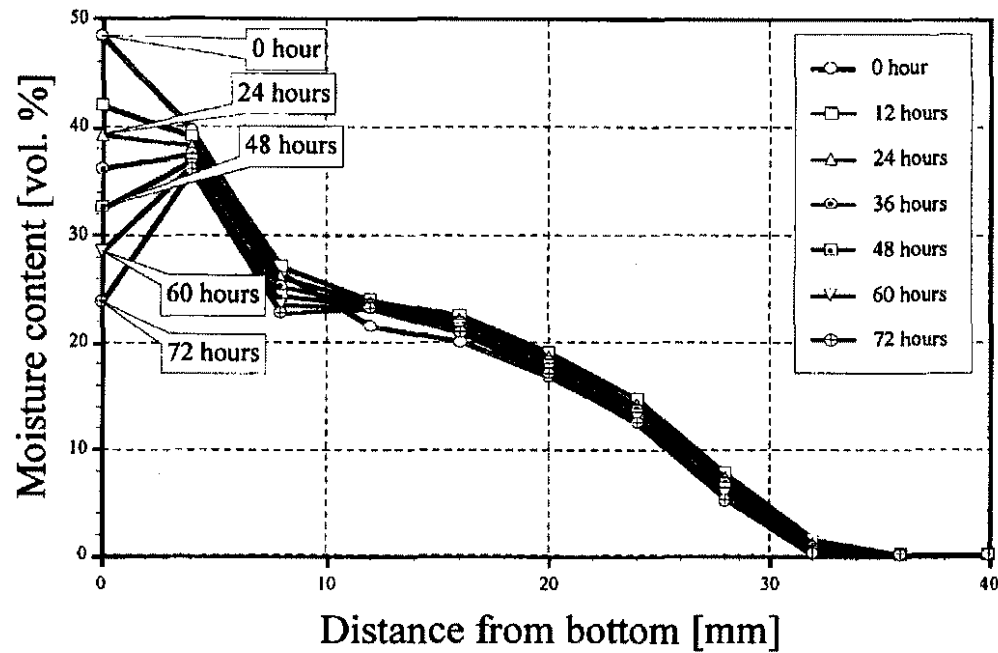
Figure 8. Calculated temperature distribution during freezing process.

well such characteristics in the measured results that the freezing proceeds from the bottom and that there is a kink in the moisture profile. However, the kink occurs around 20 mm from the bottom, while it is found at 10 mm in the measured result. Furthermore, the moisture content at the kink is 10% compared with the 20% of the measured result.

The freezing mainly occurs in a region near the bottom. The reason is as follows: the moisture moves mainly in the gaseous phase even at high moisture content since the porosity of the glass fiber is very large, 98%. As a result, no freezing is necessarily initiated at all regions where the temperature is 0°C or even lower (about 30 mm from the bottom). Instead, vapour continues to be transported to the coldest location. This is completely different from the previous result in the case of the wall made of soil [1].

Figure 8 gives the time history of the temperature distribution. The features of the measured result such as convex upward as a whole and flat near the bottom are predicted reasonably well. The convex distribution is caused by the latent heat of phase change, however, the curvature is not large compared with the measured result. This discrepancy is probably because the lateral heat flux from the sides of the sample is neglected in the one-dimensional calculation, and thus, this point is pursued in the following section.

On the other hand, the temperature distribution convex downward near the bottom region is caused by the increase in thermal conductivity with the amount of the ice.

Figure 9. *Calculated total moisture (liquid water + ice) content distribution during thawing process.*
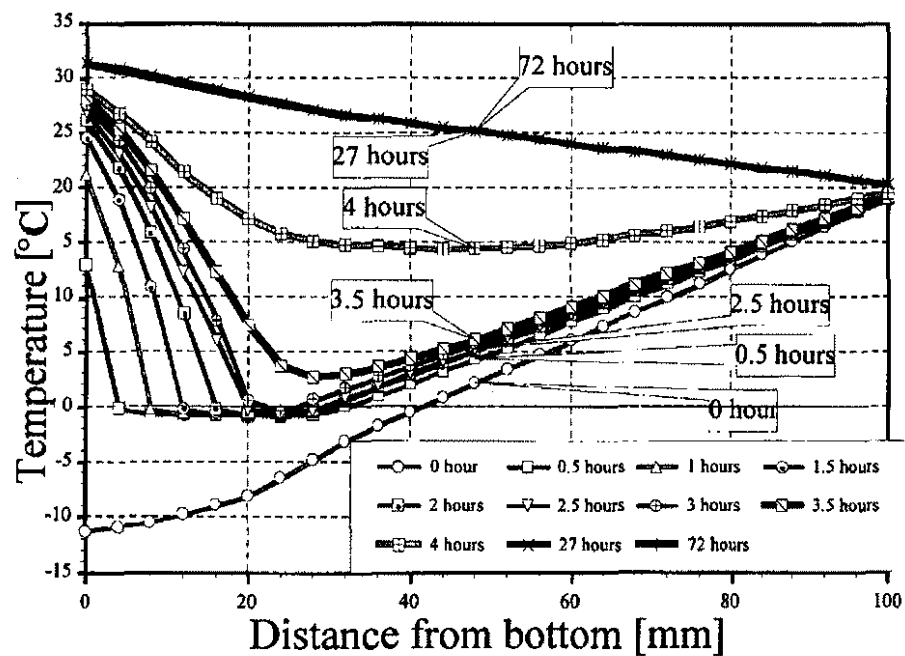
Figure 10. *Calculated temperature distribution during thawing process.*

Analysis of Thawing Process after Freezing

COMPUTATIONAL CONDITIONS

After the freezing process, the refrigerant temperature is raised to 32°C and then kept steady.

RESULTS AND DISCUSSIONS

The calculated total moisture content and temperature distributions are shown in Figures 9 and 10, respectively. By raising the temperature of the circulating refrigerant, the ice melts and evaporates from the bottom surface. The calculated moisture content agrees with the measured result in that the moisture content in the bottom region decreases much faster than in any other region and that the total amount of the moisture decreases gradually as a whole.

The calculated temperature agrees fairly well with the measured result. It remains below 0°C where the ice is found, and it increases from the bottom in sequence. However, the time required for thawing is longer than that in the experiment, partly because a role of the acrylic plate as a heat bridge is not taken into account.

TWO-DIMENSIONAL ANALYSIS

Computational Conditions

At the bottom and the upper surfaces, the same boundary conditions as in the one-dimensional calculation are used. As initial conditions, the temperatures at the upper and bottom surfaces are set at 20°C and 0°C, respectively. A linear tem-
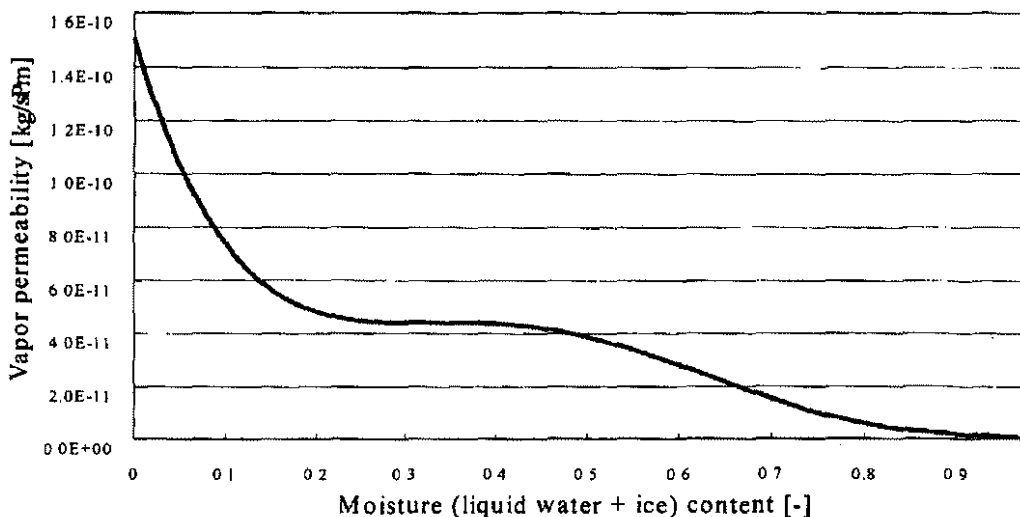

Figure 11. *Vapor permeability as function of moisture (liquid water + ice) content.*

perature profile is assumed between the two surfaces. Uniform distribution is used in the horizontal direction.

The side of the specimen was made impermeable and insulated by 19 mm thick polystyrene board in the experiment. However, the thermal resistance is optimized to a larger value = 2.03 $[m^2K/W]$ in order to obtain better agreement with the measured results in the present simulation. Also, the vapor permeability shown in Figure 11 is used in the calculation.

Results and Discussions

Figures 12 and 13 show the calculated total moisture content and temperature distributions, respectively.

The time history of the temperature distribution shown in Figure 13 predicts well the features of the measured result such as convex upward and flat near the bottom. The convex temperature distribution is partly due to the latent heat of phase change, however, the heat flux from the lateral direction can be judged as the main reason. This is evident from the fact that the temperature distribution obtained by the present two-dimensional calculation agrees well with the measured result, while the one-dimensional calculation gives an almost linear distribution.

On the other hand, the temperature distribution convex downward near the bottom region is caused by the increase in thermal conductivity with the amount of the frozen moisture. This also causes the enlargement of the frozen region and increases the temperature in the region, which agree well with the measured results in Figure 3.

As described before, a good agreement was obtained by giving the larger thermal resistance to the insulation layer (including the acrylic plate) than the design value. This seems to be mainly due to the one-dimensional treatment of the acrylic plate. Compared with the lateral heat flux from the outer air through the insulation layer, the heat flux downward through the acrylic plate has much influence on the temperature distribution in the region near the bottom, judging from the values of their thermal conductivities. This effect can be approximately taken into account by increasing the value of thermal resistance of the insulation layer at the bottom region in the one-dimensional calculations. Alternatively, a three-dimensional simulation might be required, although the effect seems much smaller compared with the introduction of two-dimensionality into one-dimensional calculation. In any case, the present program needs further improvement in order to examine these problems.

Whereas the calculated total moisture content distributions shown in Figure 12 differ slightly from the measured result in Figure 2, it predicts such characteristics that the freezing proceeds from the bottom and that there is a kink in the moisture profile.
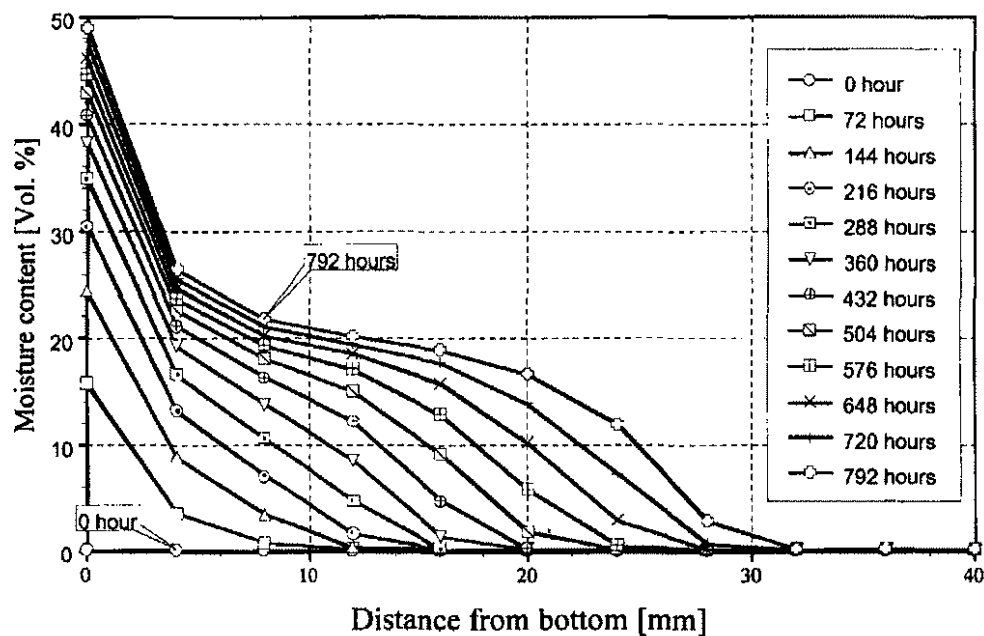
Figure 12. *Calculated total moisture (liquid water + ice) content distribution during freezing process.*
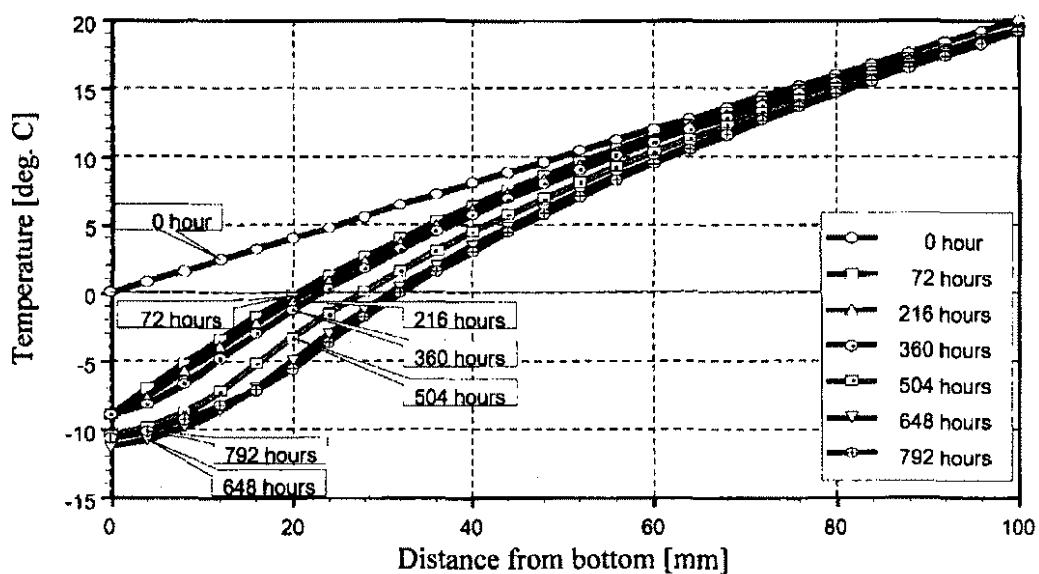

Figure 13. *Calculated temperature distribution during freezing process.*

Because the temperature at the center part of the sample in the vertical direction becomes higher due to the influence of the air temperature adjacent to the sample (Figure 15), the frozen area becomes narrower and the total amount of ice is less compared with the one-dimensional results. The position of the kink is closer to the bottom than in the one-dimensional case.

However, it must be noted that the calculated ice content became quite high in the cold regions when the original vapor permeability was used. The hygric properties used in the one-dimensional calculation are from References [9] and [10]. Because these were obtained under conditions with the temperature above the freezing point, it is not evident whether they can be used in subfreezing situations where ice may block liquid and vapor movement. The measurement of the vapor permeability under 0°C and the thorough re-examination of the present results are required, because the simulation results are highly sensitive to the value of this parameter.

By using the adjusted vapor permeability shown in Figure 11, the calculated results agree well with the measured ones, and the moisture does not concentrate near the bottom but distributes over the sample. Judging from the good agreement with the measured result, the estimation of the parameter shown in Figure 11 might be reasonable, although experimental validation is required as described before.

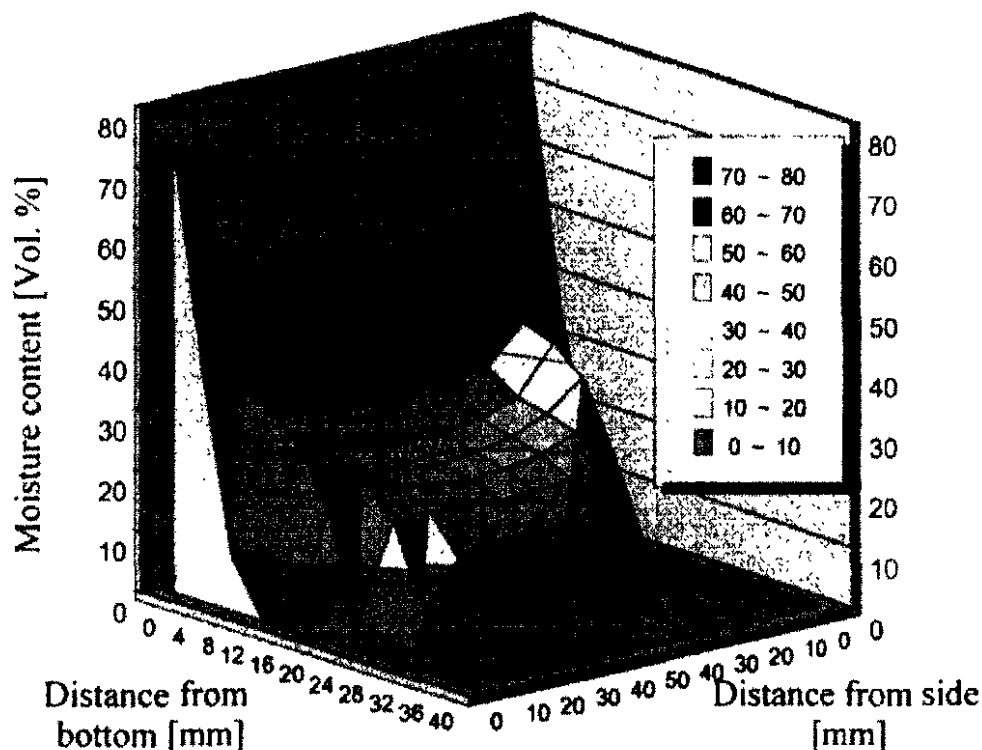Figures 14 and 15 show two-dimensional moisture content and temperature

Figure 14. Two-dimensional distribution of moisture content after 33 days (792 hours).
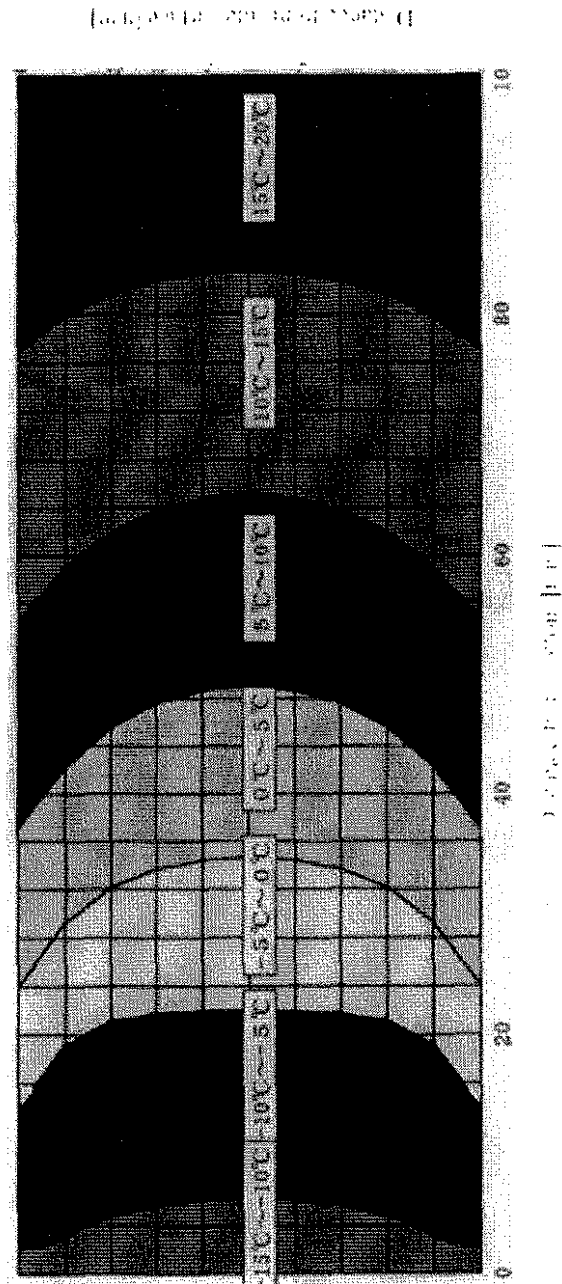
Figure 15. *Two-dimensional temperature distribution after 33 days (792 hours).*
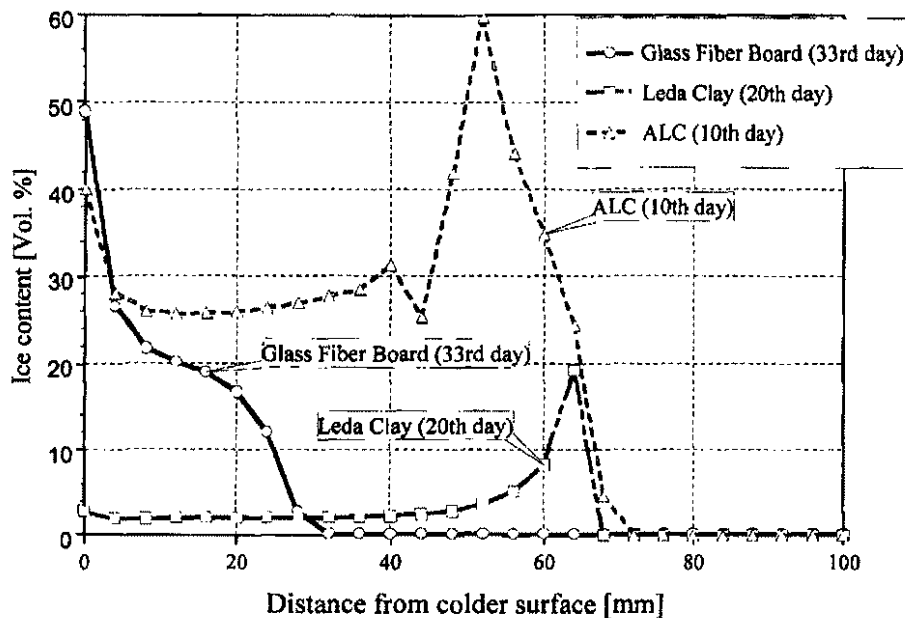
Figure 16. Ice content distribution in several building materials.

distributions, respectively. The temperature near the sample side is high as a whole compared with that inside the sample. As a result, the frozen area is limited to a narrow area close to the bottom. The maximum moisture content at the corner becomes higher than 60%. The boundary between the frozen and unfrozen areas can be found at the location where the temperature is lower than 0°C, similar to the result in one-dimensional analysis.

INFLUENCE OF TRANSPORT PROPERTIES ON FREEZING PROCESS

The ice content distributions under freezing conditions are shown in Figure 16 for several materials. These are the results calculated under constant external and internal temperatures. The wall made of glass fiber has the maximum value at the cold side where the temperature is below the freezing point, 0°C. On the other

Table 1. Effect of material properties on location of the maximum ice content.

	ALC Wall	Soil Wall (Leda Clay)	Glass Fiber Board
Porosity	70%	37.5%	98%
Moisture Transfer	Mainly in liquid phase		Mainly in gaseous phase
Position of Maximum Ice Content	Temperature 0°C		Cold edge

hand, the peaks of the ice content are found at the regions where the temperature is nearly 0°C in the walls made of ALC and soil.

Table 1 shows the relationship between the material properties and the place where the peak occurs in the ice content distribution. The peak position evidently depends on whether the moisture moves mainly in the gaseous phase or the liquid phase. While the ice concentrates at the region of the temperature below 0°C when the liquid transfer dominates, the maximum ice content occurs at the edge of the specimen with low temperature in the case of the material in which the vapor transfer is dominant. Because the moisture behavior is closely related to the porosity, it might be said that the porosity distribution has a great influence on the distribution of the ice.

CONCLUSIONS

The experiment was carried out on the freezing-thawing processes occurring in glass fiberboard. The thermal and hygric behaviors during these processes were analyzed. The freezing process was analyzed by using one- and two-dimensional equations of simultaneous heat and moisture transfer. The calculated distributions of the temperature and moisture content showed good agreement with the measured results when two-dimensional analyses were implemented. Thawing after the freezing process starts from the cold boundary and its rate is faster than that of freezing.

The hygrothermal properties such as water vapour permeability and liquid diffusivity that depend on the porosity and the hygroscopic nature of the building materials determine the location of frost development in a wall assembly. Further detailed information on transport properties such as water vapour permeability and liquid diffusivity and their dependence on temperature are needed for a more quantitative analyses of the process investigated here.

ACKNOWLEDGEMENT

REFERENCES

1. M. Hatano, S. Hokoi and M. Matsumoto: An Analysis of Freezing-thawing Processes in Building Walls, Proc. of CIB W40 meeting, Kyoto, Japan, pp.141–158, 1997.
2. M. Matsumoto and S. Ma: A Numerical Analysis for the Freezing-Melting Processes of Soils (in Japanese), J. Archi. Planning Envi. Eng., AIJ, No.482, pp.25–34, Apr., 1996.

3. A. Iwamae and M. Matsumoto: A Study on Thermal and Hygric Behavior of Snowpacks Based on Field Measurements (in Japanese), J. Archi. Planning Envi. Eng., AIJ, No.468, pp.17–25, Feb., 1995.

4. H. Chen, R. W. Besant and Y. Tao: Two-Dimensional Air Exfiltration and Heat Transfer through Fiberglass Insulation: Part 1—Numerical Model and Experimental Facility, Part 2—Comparisons between Simulations and Experiments. HVAC&R Research, Vol.3, No.3, pp.197–232, 1997.

5. A. Karagiozis, M. Salonvaara and K. Kumaran: Numerical Simulation of Experimental Freeze Conditions in Glass-Fiber Insulation, Building Physics '96—Nordic Symposium, pp.455–465, 1996.

6. ASTM Standard Test Method C666: Resistance of Concrete to Rapid Freezing and Thawing, pp.398–404, ASTM Publications, 1980.

7. M. K. Kumaran and M. Bomberg: A Gamma-Spectrometer for Determination of Density Distribution and Moisture Distribution in Building Materials, International Symposium on Moisture and Humidity, p.485, 1985.

8. M. Matsumoto, Y. Gao and S. Hokoi: Simultaneous Heat and Moisture Transfer during Freezing-Melting in Building Materials, CIB/W40 meeting in Budapest, Sept., 1993.

9. S. Hokoi and M. K. Kumaran: Experimental and Analytical Investigations of Simultaneous Heat and Moisture Transport through Glass Fiber Insulation, Journal of Thermal Insulation and Building Envelopes, Vol.16, pp.263–292, 1993.

10. M. Ohuchi, M. Matsumoto, S. Hokoi, M. K. Kumaran and R. G.Marchand: Identification of Thermal and Moisture Transport Properties of Glass Fiber Insulation, Proc. of CIB W40 meeting, Porto, Portugal, pp.178–187, 1995.